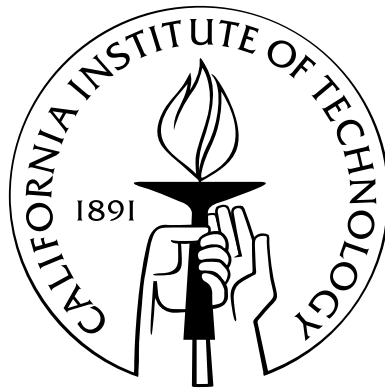


A Plasticity Model to Predict the Effects of Confinement on Concrete

Thesis by
Julie Wolf

In Partial Fulfillment of the Requirements
for the Degree of
Doctor of Philosophy



California Institute of Technology
Pasadena, California

2008
(Defended January 9, 2008)

© 2008

Julie Wolf

All Rights Reserved

Acknowledgements

I recall, while reading multiple other theses early in the course of my research, wondering why it was that people felt the need to lavishly thank all those around them at the completion of their thesis. I thought to myself, *it's a thesis, not an Academy Award!* But as I arrive (finally!) at the end of my own Ph.D., I now appreciate that this is not a journey one can complete on one's own. Without a strong network of support, I know I would never have finished. And so, I shall launch into my own 'acceptance' speech.

First, and with good reason, my family. Without you, I would never have begun such a bold undertaking and would certainly never have had the disposition, strength, and will to finish. Thanks Mom, Dad, and Lo for making me who I am (in more ways than two!).

Garrett, for putting up with me (the more realistic and less politically correct version of 'support') as I waded through my research project. The world will never know just how crazy I can be, but you always understood. You always recognized what was important to me and did everything in your power to support me in those things. I would never have survived this without you.

John Hall, for putting the idea into my head in the first place, reassuring me that I could and should get a Ph.D., and then convincing me to take on such a difficult subject matter (what was he thinking?). Aren't you glad I'm finally finished?

Anna, for the movie nights, lunches, house shopping as a couple, and general adventures that we embarked on (come on, who wouldn't want to crew for a 25 hour endurance race?). You could always be counted on to understand and sympathize with whatever mess, problem, or predicament I managed to get myself into, and to

jump into whatever harebrained adventure I was trying at the moment. You were always a shoulder to cry on, an ear to vent to, and a pair of eyes to read about the fascinating subject of concrete plasticity. You're probably the only person who is more sick of my thesis than I am!

Laura, for always understanding, never judging, patiently listening, and being one of the best examples I've found of exactly who I want to be.

Patrick, for being the only other person alive (or dead, for that matter) to read every single word of this thesis, the only person willing to debate the use of single versus double quotes into the wee hours of the morning, for teaching me about Oxford commas, semi-colon use, and the glories of the English language (as only an Englishman can do). I thank you for being there at 4 a.m. when the world was on fire, and, just as important, when it wasn't. Oh yeah, and thanks for teaching me how to drive (and we both know what *that* entailed)!

Sue, for being my home away from it all, for showing me a path when I was hopelessly lost and then getting me onto it, and for reminding me that there is a lot more to life than thesis research (shocking, I know). And, of course, teaching me how to not die on a cross country course, and maybe even have a little fun doing it!

Sherpa (your spirit will always be with me in every horse I ride), First Mate, Brushfire, and Cally. Without you all, I would surely have lost my sanity. You have so much to teach us all about how we should live and what's really important (which, as we all know, is carrots!).

Jasmine, because I may be the only person, ever, to dedicate their thesis to a car (have I mentioned the insanity?). As with the horses, you helped keep me sane (well, my version of sane), reminded me of the joys of thinking hard about physics and dynamics (yes, mid-engine cars *are* hard to drive), gave me rewards when I so desperately needed them, and didn't kill me when I messed up (though, clearly, you thought about it).

And last, but not least, I would like to thank the Academy for this award. Oh, wait a minute . . .

Abstract

A plasticity model to predict the behavior of confined concrete is developed. The model is designed to implicitly account for the increase in strength and ductility due to confining a concrete member. The concrete model is implemented into a finite element (FE) model. By implicitly including the change in the strength and ductility in the material model, the confining material can be explicitly included in the FE model. Any confining material can be considered, and the effects on the concrete of failure in the confinement material can be modeled. Test data from a wide variety of different concretes utilizing different confinement methods are used to estimate the model parameters. This allows the FE model to capture the generalized behavior of concrete under multiaxial loading. The FE model is used to predict the results of tests on reinforced concrete members confined by steel hoops and fiber reinforced polymer (FRP) jackets. Loading includes pure axial load and axial load-moment combinations. Variability in the test data makes the model predictions difficult to compare but, overall, the FE model is able to capture the effects of confinement on concrete. Finally, the FE model is used to compare the performance of steel hoop to FRP confined sections, and of square to circular cross sections. As expected, circular sections are better able to engage the confining material, leading to higher strengths. However, higher strains are seen in the confining material for the circular sections. This leads to failure at lower axial strain levels in the case of the FRP confined sections. Significant differences are seen in the behavior of FRP confined members and steel hoop confined members. Failure in the FRP members is always determined by rupture in the composite jacket. As a result, the FRP members continue to take load up to failure. In contrast, the steel hoop confined sections exhibit extensive strain

softening before failure. This comparison illustrates the usefulness of the concrete model as a tool for designers. Overall, the concrete model provides a flexible and powerful method to predict the performance of confined concrete.

Contents

| | |
|--|------------|
| Acknowledgements | iii |
| Abstract | v |
| 1 Introduction | 1 |
| 2 Plasticity Review | 5 |
| 2.1 Stress Invariants | 5 |
| 2.2 Failure Surface | 9 |
| 2.3 Plastic Flow | 11 |
| 2.4 Consistency Condition | 12 |
| 3 Model Definition | 14 |
| 3.1 Loading Surfaces | 16 |
| 3.1.1 Meridians | 17 |
| 3.1.2 Elliptic Fit | 20 |
| 3.2 Failure Surface | 21 |
| 3.3 Flow Rule | 23 |
| 3.4 Model Parameters | 24 |
| 3.5 Tangent Modulus Tensor | 25 |
| 4 Model Identification | 27 |
| 4.1 Yield Surface Definition | 28 |
| 4.2 Peak Surface Correlation | 30 |
| 4.2.1 Peak Surface Papers | 31 |

| | | |
|----------|--|-----------|
| 4.2.1.1 | Peak Surface Papers Utilizing a Triaxial Pressure Vessel | 34 |
| 4.2.1.2 | Peak Surface Papers Utilizing a True Triaxial Testing Machine | 39 |
| 4.2.1.3 | Peak Surface Papers Utilizing Passive Confinement . | 41 |
| 4.2.1.4 | Peak Surface Papers Utilizing Biaxial Loading | 42 |
| 4.2.2 | Peak Surface Data | 43 |
| 4.2.3 | Peak Surface Fit | 49 |
| 4.3 | Residual Surface Correlation | 55 |
| 4.3.1 | Residual Surface Papers | 57 |
| 4.3.2 | Residual Surface Data | 59 |
| 4.3.3 | Residual Surface Fit | 60 |
| 4.4 | Determination of the Equation for the Damage Increment | 62 |
| 4.4.1 | Papers Used to Determine the Equation for the Damage Incre- ment | 64 |
| 4.4.2 | Discussion of Test Data Used to Determine the Equation for the Damage Increment | 65 |
| 4.5 | Correlation of the Failure Surface and Flow Rule Parameters | 71 |
| 4.6 | Summary of Parameters | 76 |
| 5 | Finite Element Program | 77 |
| 6 | Comparisons to Tests on Reinforced Concrete Members | 82 |
| 6.1 | Test Data | 82 |
| 6.2 | Comparison Results | 86 |
| 6.2.1 | Chaallal and Shahawy (2000) | 86 |
| 6.2.2 | Harries and Carey (2003) | 87 |
| 6.2.3 | Harries and Kharel (2003) | 89 |
| 6.2.4 | Mander et al. (1988a) | 93 |
| 6.2.5 | Scott et al. (1982) | 99 |
| 6.3 | Conclusions from the Comparisons | 103 |

| | | |
|----------|---|------------|
| 7 | Effects of Cross Sectional Shape and Confining Material | 106 |
| 7.1 | Discussion of Sections Used for Performance Comparison | 107 |
| 7.2 | Results of Comparison | 108 |
| 7.2.1 | Axial Load Performance Comparison | 109 |
| 7.2.2 | Axial Load-Moment Performance Comparison | 112 |
| 8 | Conclusions | 118 |
| A | Partial Derivatives Required for Equation 3.14 | 128 |
| B | Summary of Papers Used for Determining Peak Surface Parameters | 134 |
| C | Figures Showing Individual Data Sets for Papers Used to Determine Peak Surface | 139 |
| D | Summary of Papers Used for Determining Residual Surface Parameters | 150 |
| E | Fortran Code of the Finite Element Program Containing the Concrete Plasticity Model | 152 |
| F | Summary of Papers Used for Validating the Model | 200 |
| G | Finite Element Meshes Used for Comparisons to Tests on Reinforced Concrete Members | 202 |
| G.1 | Chaallal and Shahawy (2000) | 203 |
| G.2 | Harries and Carey (2003) | 204 |
| G.3 | Harries and Kharel (2003) | 206 |
| G.4 | Mander et al. (1988a) | 206 |
| G.5 | Scott et al. (1982) | 209 |
| H | Finite Element Meshes Used for Effects of Cross Sectional Shape and Confining Material | 211 |

List of Figures

| | | |
|-----|---|----|
| 2.1 | Graphical interpretation of stress invariants (ξ, r, θ) in the principal stress space. | 8 |
| 3.1 | Location of loading surfaces on a uniaxial stress strain curve. | 16 |
| 3.2 | Shape of the peak and residual tensile and compressive meridians in the (ξ, r) space. | 18 |
| 3.3 | Shape of the yield tensile and compressive meridians in the (ξ, r) space. | 19 |
| 3.4 | Elliptic trace of the failure surface for $0^\circ \leq \theta \leq 60^\circ$ | 20 |
| 3.5 | Deviatoric section of the failure surface. | 21 |
| 3.6 | Graphical representation of the direction of plastic flow depending on ω based on Noble et al. (2005). | 23 |
| 4.1 | Example of a triaxial pressure vessel. Reproduced from Imran and Pantazopoulou (1996). | 32 |
| 4.2 | Example of a true triaxial testing machine. Reproduced from Launay and Gachon (1972a). | 33 |
| 4.3 | Test data for peak compressive and tensile meridians. | 43 |
| 4.4 | Test data for peak compressive and tensile meridians: low confinement region. | 44 |
| 4.5 | Change in the effectiveness of confinement with concrete compressive strength. | 45 |
| 4.6 | Change in the effectiveness of confinement with concrete compressive strength: low confinement region. | 46 |

| | | |
|------|---|----|
| 4.7 | Change in the effectiveness of confinement with the confinement method: low confinement region. | 47 |
| 4.8 | Change in the effectiveness of confinement with specimen size: low con- finement region. | 47 |
| 4.9 | Change in the effectiveness of confinement with year of experiment. . . | 48 |
| 4.10 | Change in the effectiveness of confinement with era of experiment: low confinement region. | 49 |
| 4.11 | Shape of the test data in the (r, θ) plane. | 50 |
| 4.12 | Peak compressive and tensile meridians for fit of all data. | 52 |
| 4.13 | Peak compressive and tensile meridians for fit of all data: low confine- ment region. | 52 |
| 4.14 | Comparison of peak compressive and tensile meridians for two different fits. | 54 |
| 4.15 | Comparison of peak compressive and tensile meridians for two different fits: low confinement region. | 54 |
| 4.16 | Comparison of peak compressive meridian to existing models. | 56 |
| 4.17 | Comparison of peak compressive meridian to existing models: low con- finement region. | 56 |
| 4.18 | Test data for residual compressive meridian. | 60 |
| 4.19 | Fit for residual compressive meridian with no constraints on the param- eters. | 61 |
| 4.20 | Final fit for the residual surface compressive meridian. | 63 |
| 4.21 | Variation of strain at unconfined peak stress with concrete compressive strength, f'_c | 66 |
| 4.22 | Ratio of confined strain to unconfined strain at peak stress plotted versus ξ | 67 |
| 4.23 | Ratio of confined strain to unconfined strain at peak stress plotted versus $\xi/\sqrt{f'_c}$ | 68 |
| 4.24 | Ratio of confined strain to unconfined strain at peak stress plotted versus ξ/f'_c | 69 |

| | | |
|------|---|----|
| 4.25 | Power law fit for ratio of confined strain to unconfined strain at peak stress versus ξ/f'_c | 69 |
| 4.26 | Test data for 5.0 ksi (34.5 MPa) concrete from Smith et al. (1989). . . | 73 |
| 4.27 | Test data for 6.1 ksi (41.9 MPa) concrete from Candappa et al. (1999) and Candappa et al. (2001). | 73 |
| 4.28 | Comparison of model to data from Smith et al. (1989). | 75 |
| 4.29 | Comparison of model to data from Candappa et al. (1999) and Candappa et al. (2001). | 75 |
| 5.1 | Typical slice of column used for FE model. | 78 |
| 5.2 | Typical mesh used for circular cross sections. | 79 |
| 5.3 | Comparable meshes with steel hoops versus FRP confinement. | 80 |
| 6.1 | Comparison of model to test data from Chaallal and Shahawy (2000). . | 86 |
| 6.2 | Comparison of model to test data from Harries and Carey (2003) for circular column. | 88 |
| 6.3 | Comparison of model to test data from Harries and Carey (2003) for square column with 0.43 inch (11 mm) corner radius. | 88 |
| 6.4 | Comparison of model to test data from Harries and Carey (2003) for square column with 0.98 inch (25 mm) corner radius. | 89 |
| 6.5 | Axial stress versus strain comparison of model to test data from Harries and Kharel (2003) for columns confined by carbon FRP. | 90 |
| 6.6 | Dilation ratio comparison of model to test data from Harries and Kharel (2003) for columns confined by carbon FRP. | 90 |
| 6.7 | Axial stress versus strain comparison of model to test data from Harries and Kharel (2003) for columns confined by E-glass FRP. | 91 |
| 6.8 | Dilation ratio comparison of model to test data from Harries and Kharel (2003) for columns confined by E-glass FRP. | 92 |
| 6.9 | Details of circular columns tested in Mander et al. (1988a) and predicted using the current model. | 93 |

| | | |
|------|--|-----|
| 6.10 | Comparison of model to test data from Mander et al. (1988a) for circular columns. | 94 |
| 6.11 | Comparison of model with round residual surface to test data from Mander et al. (1988a) for circular columns. | 95 |
| 6.12 | Comparison of FE model to test data from Mander et al. (1988a) for column 4. | 96 |
| 6.13 | Details of rectangular walls tested in Mander et al. (1988a) and predicted using the current model. | 97 |
| 6.14 | Comparison of model to test data from Mander et al. (1988a) for rectangular walls. | 98 |
| 6.15 | Comparison of model with round residual surface to test data from Mander et al. (1988a) for rectangular walls. | 98 |
| 6.16 | Details of square columns tested in Scott et al. (1982) and predicted using the current model. | 99 |
| 6.17 | Comparison of model to test data from Scott et al. (1982) for square columns. | 100 |
| 6.18 | Comparison of model with round residual surface to test data from Scott et al. (1982) for square columns. | 101 |
| 6.19 | Comparison of model to test data from Scott et al. (1982) for column 2 concrete and steel forces. | 101 |
| 6.20 | Comparison of model to test data from Scott et al. (1982) for column 2 hoop stresses. | 102 |
| 6.21 | Comparison of model to test data from Scott et al. (1982) for column 6 concrete and steel forces. | 102 |
| 6.22 | Comparison of model to test data from Scott et al. (1982) for column 6 hoop stresses. | 103 |
| 7.1 | Details of square and circular cross sections confined by steel hoops. . . | 107 |
| 7.2 | Comparison of the axial performance of steel confined sections. | 109 |
| 7.3 | Comparison of the axial performance of E-glass confined sections. . . . | 110 |

| | | |
|------|--|-----|
| 7.4 | Axial load-moment interaction diagram for all four different sections. . . | 112 |
| 7.5 | Normalized axial load-moment interaction diagram for all four different sections. | 114 |
| 7.6 | Moment versus curvature curves for the steel confined circular cross section. | 115 |
| 7.7 | Moment versus curvature curves for the steel confined square cross section. | 115 |
| 7.8 | Moment versus curvature curves for the E-glass FRP confined circular cross section. | 116 |
| 7.9 | Moment versus curvature curves for the E-glass FRP confined square cross section. | 116 |
| C.1 | Test data from Ahmad and Shah (1982). | 139 |
| C.2 | Test data from Ansari and Li (1998), Li and Ansari (1999), and Li and Ansari (2000). | 140 |
| C.3 | Test data from Attard and Setunge (1996). | 140 |
| C.4 | Test data from Balmer (1949). | 141 |
| C.5 | Test data from Bellamy (1961). | 141 |
| C.6 | Test data from Calixto (2002). | 142 |
| C.7 | Test data from Candappa et al. (1999) and Candappa et al. (2001). . . | 142 |
| C.8 | Test data from Chinn and Zimmerman (1965). | 143 |
| C.9 | Test data from Chuan-zhi et al. (1987). | 143 |
| C.10 | Test data from Cordon and Gillespie (1963). | 144 |
| C.11 | Test data from Duke and Davis (1944). | 144 |
| C.12 | Test data from Imran and Pantazopoulou (1996). | 145 |
| C.13 | Test data from Kupfer et al. (1969) and Kupfer and Gerstle (1973). . . | 145 |
| C.14 | Test data from Lan and Guo (1997). | 146 |
| C.15 | Test data from Launay and Gachon (1972a) and Launay and Gachon (1972b). | 146 |
| C.16 | Test data from Mills and Zimmerman (1970). | 147 |
| C.17 | Test data from Richart et al. (1928). | 147 |

| | | |
|------|--|-----|
| C.18 | Test data from Richart et al. (1929). | 148 |
| C.19 | Test data from Rosenthal and Glucklich (1970). | 148 |
| C.20 | Test data from Sfer et al. (2002). | 149 |
| C.21 | Test data from Toutanji (1999). | 149 |
| G.1 | Finite element representation of member tested in Chaallal and Shahawy (2000). | 203 |
| G.2 | Finite element representation of member with circular cross section tested in Harries and Carey (2003). | 204 |
| G.3 | Finite element representation of member with square cross section and 0.43 inch (11 mm) corner radius tested in Harries and Carey (2003). . . | 205 |
| G.4 | Finite element representation of member with square cross section and 0.98 inch (25 mm) corner radius tested in Harries and Carey (2003). . . | 205 |
| G.5 | Finite element representation of column 1 tested in Mander et al. (1988a). | 206 |
| G.6 | Finite element representation of columns 2-4 tested in Mander et al. (1988a). | 207 |
| G.7 | Finite element representation of walls 1, 3, and 4 tested in Mander et al. (1988a). | 208 |
| G.8 | Finite element representation of column 2 tested in Scott et al. (1982). | 209 |
| G.9 | Finite element representation of column 6 tested in Scott et al. (1982). | 210 |
| H.1 | Finite element representation of square column confined by steel hoops, used for comparison in Chapter 7. | 212 |
| H.2 | Finite element representation of circular column confined by steel hoops, used for comparison in Chapter 7. | 213 |
| H.3 | Finite element representation of square column confined by FRP, used for comparison in Chapter 7. | 214 |
| H.4 | Finite element representation of circular column confined by FRP, used for comparison in Chapter 7. | 215 |
| H.5 | Finite element representation of square column confined by FRP, used for special load cases of comparison in Chapter 7. | 216 |

List of Tables

| | | |
|-----|--|-----|
| 3.1 | Summary of model parameters. | 24 |
| 4.1 | Peak surface parameters for fit of all data. | 51 |
| 4.2 | Peak surface parameters for low confinement range. | 53 |
| 4.3 | Residual surface parameters. | 62 |
| 4.4 | Smith et al. (1989) raw data points. | 70 |
| 4.5 | Summary of failure surface and flow rule parameter values. | 74 |
| 4.6 | Summary of model parameter values. | 76 |
| 7.1 | Confinement equivalence by elastic stiffness. | 108 |
| 7.2 | Strength and ductility comparison of square versus circular steel confined sections. | 111 |
| B.1 | Summary of papers used for determining peak surface parameters. . . . | 135 |
| B.1 | Summary of papers used for determining peak surface parameters. . . . | 136 |
| B.1 | Summary of papers used for determining peak surface parameters. . . . | 137 |
| B.1 | Summary of papers used for determining peak surface parameters. . . . | 138 |
| D.1 | Summary of papers used for determining residual surface parameters. . . | 151 |
| F.1 | Summary of papers used for validating the model. | 201 |

Table of Variables

| Variable | Definition | Location |
|---|---|---------------|
| $a_{0,peak}, a_{1,peak},$ $a_{2,peak}, a_{3,peak}$ | parameters defining the peak tensile meridian | Equation 3.1 |
| $b_{0,peak}, b_{1,peak},$ $b_{2,peak}, b_{3,peak}$ | parameters defining the peak compressive meridian | Equation 3.1 |
| $a_{0,residual},$ $a_{1,residual},$ $a_{2,residual},$ $a_{3,residual}$ | parameters defining the residual tensile meridian | Equation 3.1 |
| $b_{0,residual},$ $b_{1,residual},$ $b_{2,residual},$ $b_{3,residual}$ | parameters defining the residual compressive meridian | Equation 3.1 |
| c | parameter defining the yield tensile meridian | Equation 3.2 |
| D_{ijkl}^e | material elastic modulus tensor | Section 2.3 |
| D_{ijkl}^p | material plastic modulus tensor | Equation 3.14 |
| $D_{ijkl}^{tangent}$ | material tangent modulus tensor | Equation 3.13 |
| d | parameter defining the yield compressive meridian | Equation 3.2 |
| $d\epsilon_{ij}$ | total strain increment | Equation 2.14 |
| $d\epsilon_{ij}^p$ | plastic strain increment | Equation 2.14 |
| $\overline{d\epsilon^p}$ | effective plastic strain increment | Equation 2.17 |

| | | |
|-----------------------------|---|---------------------------|
| $d\lambda$ | positive scalar factor of proportionality, used for plastic flow definition | Equation 3.12 |
| $d\sigma_{ij}$ | elastic stress increment | Equation 3.10 |
| $d\psi$ | damage increment | Equation 3.5 |
| E | modulus of elasticity | Section 3.4 |
| F | failure surface | Section 2.2 |
| F_{peak} | peak loading surface | Equation 3.4 |
| $F_{residual}$ | residual loading surface | Equation 3.4 |
| F_{yield} | yield loading surface | Equation 3.4 |
| f'_c | unconfined concrete compressive strength | Section 3.1.1 |
| I_1, I_2, I_3 | first, second, and third invariants of the stress tensor | Equations 2.5 through 2.7 |
| J_2, J_3 | second and third invariants of the deviatoric stress tensor | Equation 2.8 and 2.9 |
| Q | potential surface | Section 3.3 |
| $R_{peak}(\xi, \theta)$ | cross section of the peak loading surface in the deviatoric plane | Equation 3.3 |
| $R_{residual}(\xi, \theta)$ | cross section of the residual loading surface in the deviatoric plane | Equation 3.3 |
| $R_{yield}(\xi, \theta)$ | cross section of the yield loading surface in the deviatoric plane | Equation 3.3 |
| r | deviatoric length invariant | Equation 2.11 |
| $r_{c,peak}$ | compression meridian of the peak loading surface | Equation 3.1 |
| $r_{c,residual}$ | compression meridian of the residual loading surface | Equation 3.1 |
| $r_{c,yield}$ | compression meridian of the yield loading surface | Equation 3.2 |
| $r_{t,peak}$ | tensile meridian of the peak loading surface | Equation 3.1 |
| $r_{t,residual}$ | tensile meridian of the residual loading surface | Equation 3.1 |

| | | |
|--------------------------------|--|---------------|
| $r_{t,yield}$ | tensile meridian of the yield loading surface | Equation 3.2 |
| s_{ij} | deviatoric stress tensor | Equation 2.3 |
| α, γ | parameters controlling the effect of confinement on damage accumulation | Equation 3.5 |
| β | defines the location of the failure surface relative to the loading surface | Equation 3.7 |
| ϵ_{ij}^e | total elastic strain | Equation 2.16 |
| ϵ_{ij} | total strain | Equation 2.15 |
| ϵ_{ij}^p | total plastic strain | Section 2.3 |
| θ | Lode angle or angle of similarity | Equation 2.12 |
| κ | parameter controlling the rate of travel of the failure surface from one loading surface to the next | Equation 3.7 |
| ν | Poisson's ratio | Section 3.4 |
| ξ | hydrostatic length invariant | Equation 2.10 |
| σ_{ij} | stress tensor | Equation 2.1 |
| $\sigma_1, \sigma_2, \sigma_3$ | principal stress invariants | Section 2.1 |
| ϕ | parameter controlling damage accumulation at low stress levels | Equation 3.5 |
| ψ | current damage level | Section 3.2 |
| ψ_{peak} | damage level corresponding to the peak stress state | Section 3.2 |
| ω | parameter controlling the amount of plastic volume change | Figure 3.6 |